Kinetik: Game Technology, Information System, Computer Network, Computing, Electronics, and Control
Journal homepage: http://kinetik.umm.ac.id
ISSN: 2503-2267
Vol. 10, No. 1, February, Pp. 37-46

Design and implementation of two-phase boost inverter using interleaved method to increase output current

Fahrul Indra Setiyawan*[1], Leonardus Heru Pratomo[1]
Electrical Engineering Department, Soegijapranata Catholic University, Indonesia[1]

Article Info
Keywords:
Renewable Energy, Two Phase Interleaved Boost Converter, Current Controlled, THD

Article history:
Received: June 28, 2024
Accepted: October 03, 2024
Published: February 01, 2025

Cite:
F. I. Setiyawan and L. H. . Pratomo, "Design and Implementation of Two-phase Boost Inverter using Interleaved Method to Increase Output Current", *KINETIK*, vol. 10, no. 1, Feb. 2025.
https://doi.org/10.22219/kinetik.v10i1.2046

*Corresponding author.
Fahrul Indra Setiyawan
E-mail address:
fahrulindra09@gmail.com

Abstract
The advancement of technology is rapidly evolving, particularly in the field of electronics, namely power electronics. One of the applications is the use of new and renewable energy. The converters required in new and renewable energy are inverters with good quality and performance. The step-down (buck) inverter is commonly used in this application. Different from the normal inverter, the step up (boost) inverter is proposed to be analyzed, simulated, and implemented in this paper. The proposed inverter uses a two-phase interleaved boost inverter (TP DC-AC IBI) consisting of a full bridge inverter and dual AC-AC interleaved boost converter. The inverter part always converts DC voltage to AC voltage, while the dual AC-AC interleaved boost converter part serves to increase the output voltage. The inverter consists of three arms: the first and second arms are controlled by Sinusoidal Pulse Width Modulation (SPWM) using 180° phase-shifted carrier signal, and the third arm is controlled by a zero-crossing detector. Pulse Width Modulation (PWM) is used to control dual AC-AC interleaved boost converter. By combining this inverter with dual AC-AC interleaved boost converter, a new topology is created. This study specifically investigated the strategy to control this new topology using current controls. The actual current was obtained by installing an HX-10P current sensor on the output side. The output current was compared with the reference current, and the next stage was controlled using a proportional plus integral controller. The control signals output was modulated using SPWM signals on the inverter side and PWM at the AC-AC interleaved boost converter side to drive many power switches. To guarantee that the desired current control can always be achieved, the actual current and reference current must always match. The proportional plus integral controller was chosen due to its simplicity, high accuracy, and quick response time. The analysis involved verifying simulation tests using Power Simulator (PSIM) software. The hardware implementation was conducted in the laboratory and tested using standardized equipment. A couple of inductors were installed to reduce harmonic current on the output side and obtained THD of 3.3%, which according to the IEEE 519-2014, has met the standard as it was less than 5%. Thus, this new topology can be used in new and renewable energy for its good performance.

1. Introduction

Injecting current into the grid with a single-phase inverter is an example of applying an inverter, where a low harmonic inverter is needed because the harmonic in the output current affects the quality of the current that will be injected into the grid [1], [2]. Most inverters available on the market nowadays have high THD, which can affect the quality of the current they produce [3]. Therefore, many types of inverters have now been developed, one of which is a current-controlled inverter with the aim of being able to produce an output current with low THD. Apart from that, the use of renewable energy is increasingly popular, urging the need to develop the inverters and other converters. [4]. The use of Photovoltaic (PV), wind power, and hydro-power is currently becoming a trend as an environmentally friendly energy source, and the amount is unlimited [5], [6]. Consequently, the use of fossil fuels is slowly starting to be abandoned [7]. Almost the entire world uses energy derived from fossil fuels [8], [9]. This has an effect on the amount of availability which decreases as time goes by [10]. Despite being non-renewable, this energy source also has a negative impact on the environment, namely producing air pollution [11], [12]. Renewable energy is one solution to overcome this problem. The reason for using renewable energy is that it does not produce gas emissions and is easy to apply, making renewable energy the right choice for now and the future [13], [14].

Similar to fossil fuels, to produce energy for general use, a renewable energy also requires a system in the form of an inverter or converter [15], [16]. The use of this system functions to facilitate the use of renewable energy sources

and achieve the expected results [17], [18]. This paper will discuss Two-Phase Interleaved Boost Inverter (TP DC – AC IBI). TP DC – AC IBI is capable of producing large power with controlled current, the THD on the output current side is quite low. TP DC – AC IBI is the result of combining an inverter with an AC – AC boost converter. TP DC - AC IBI can be used in renewable energy applications because the output from the renewable energy such as PV, hydroelectric power plants, and wind power plants is in the form of DC voltage, which is then fed into the TP DC – AC IBI, causing large power production and low THD current. Therefore, when the current is injected into the grid, it has good quality. In a system, the harmonic value is always minimized so that it can be as low as possible, even down to zero [19], [20]. TP DC – IBI AC is suitable for use at high power. THD can be reduced by dividing the current equally between the two converters. The use of interleaved topology is to reduce losses in the boost section [21]. Another function is to help overcome harmonic problems in the output current [22]-[24].

This research investigated the new topology of an inverter, called TP DC - AC IBI. The inverter was commonly used in application for current or voltage control strategy. Based on the application, the paper investigated TP DC - AC IBI with output current control output strategy. This method always maintains the output current with the desire current reference using proportional integral controller. TP DC - AC IBI was tested using two methods: simulation testing with the help of Power Simulator (PSIM) software and direct testing in the laboratory. The details of the TP DC – AC IBI design was further explained in section 2, the results and discussion related to the TP DC – AC IBI are described in section 3, and in section 4, the conclusion regarding the tests that have been carried out using computational simulations and hardware implementation in the laboratory is presented.

2. Research Method

2.1 DC – DC Interleaved Boost Converter

An interleaved boost converter (IBC) is two conventional boost circuits connected into one. The working principle of the boost converter is to increase the output power produced. This boost converter works by regulating the power switch using PWM (pulse width modulation). Figure 1 shows the shape of the IBC topology. The DC-DC IBC circuit can be analyzed when *the switch* is closed (on) and *the switch* is open (off).

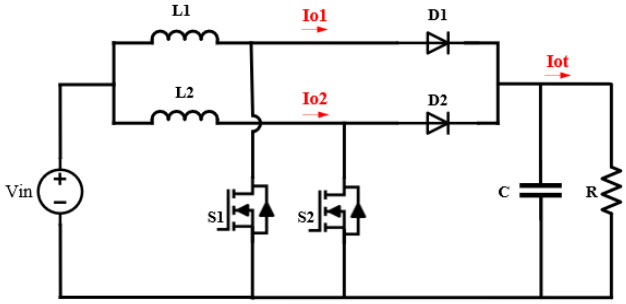

Figure 1. Conventional DC – DC Boost Converter

The DC-DC IBC circuit has four operating modes, the following are the operating modes in the DC-DC IBC circuit:

- The first operating mode applies when power switches S1 and S2 are active. Current flows from the DC input to the inductors L1 and L2. At that time the voltage in inductors L1 and L2 will be the same as the DC input voltage (Vin), so that Equation 1 and Equation 2 are obtained.

$$V_{in} = V_{L1} = L1\frac{di}{dt} \quad (1)$$

$$V_{in} = V_{L2} = L2\frac{di}{dt} \quad (2)$$

- The second operating mode has two conditions: the first condition is when the power switch S1 is off. The second condition is when switch S2 is active. In the first condition, the voltage on inductor L2 will be the same as the DC input voltage (Vin), while in the second condition the DC input voltage (Vin) plus inductor L1 will be pushed to the output side. In mathematical terms, when the first condition applies, the Equation 3 is used:

$$V_{in} = V_{L2} = L2\frac{di}{dt} \quad (3)$$

Meanwhile, Equation 4 is the mathematical modeling for the second condition:

$$V_{in} + V_{L1} = V_o \quad (4)$$

- The third operating mode also has two conditions: the first condition is when the power switch S2 is off. The second condition is when switch S1 is active. In the first condition, the voltage on inductor L1 will be the same as the DC input voltage (Vin), while in the second condition, the DC input voltage (Vin) plus inductor L2 will be pushed to the output side. In mathematical terms, when the first condition applies Equation 5 is used:

$$V_{in} = V_{L1} = L1\frac{di}{dt} \quad (5)$$

Meanwhile, Equation 6 is applied to the second condition:

$$V_{in} + V_{L2} = V_o \quad (6)$$

- The fourth operating mode applies when power switches S1 and S2 are inactive. The DC input voltage (Vin) plus the voltage of inductors L1 and L2 will be driven to the output side. In mathematical terms, Equation 7 and Equation 8 are used:

$$V_{in} + V_{L1} = V_o \quad (7)$$

$$V_{in} + V_{L2} = V_o \quad (8)$$

Equations (1) – (8) can be derived from the output voltage equation to the input voltage as a function of the duty cycle.

$$V_o = \frac{1}{1-D} V_{in} \quad (9)$$

The output power equation can be derived as follows:

$$\mathbf{Po_{inv} = (I_{L1} + I_{L2})\, R} \quad (10)$$

From Equation 9, it can be seen that by controlling two arms using the carrier signal shifted by 180°, the power on the output side will increase twice and the current on the output side will be reduced by 50%.

2.2 Inverter

A three-arm inverter is used as equipment to implement TP DC – AC IBI using an MOSFET as a power switch, as presented in Figure 2. On both arms, there is a power switch that alternately switches S1 with S2, then S3 with S4. Each arm is controlled by a 180° phase-shifted carrier signal. The third arm is controlled by detecting positive and negative cycles (Z_{C1} and Z_{C2}), better known as zero crossing detector. S1 and S2 are one arm and connected to inductor 1 (L1), while S3 and S4 are two arms connected to inductor 2 (L2). In general, the inverter output voltage is calculated by using Equation 11:

$$\mathbf{Vo\_inv = m\ Dc} \quad (11)$$

Where *m* is the modulation index which is the ratio of the sinusoidal wave voltage and the carrier voltage (triangle).

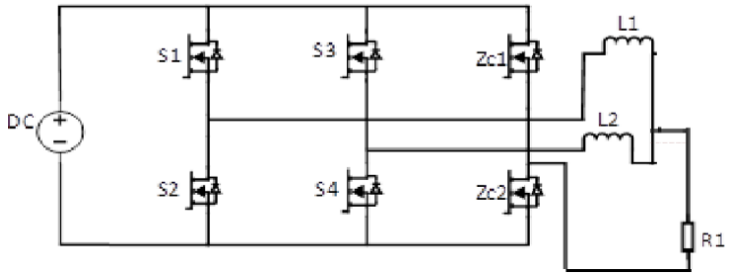

Figure 2. Two Phase Three Arm Inverter

The following is a complete table of inverter operating modes during the positive cycle, presented in Table 1.

Table 1. Two - Phase Full Bridge Inverter Switching Pattern

Mode	S1	S2	S3	S4	Zc1	Zc2	Vo
1	1	0	1	0	0	1	E
2	1	0	0	0	0	1	E
3	0	0	1	0	0	1	E
4	0	0	1	1	0	1	0 “Freewheeling DS2 DS4”
5	0	0	0	1	0	1	0 “Freewheeling DS4”
6	0	0	1	0	0	1	0 “Freewheeling DS2”

2.3 Two Phase Interleaved Boost Inverter

Three-arm inverter and AC – AC IBC are combined to create TP DC – AC IBI circuit. The power circuit is as shown in Figure 3, where the left side is the three-arm inverter section, and the right side is the AC – AC IBC.

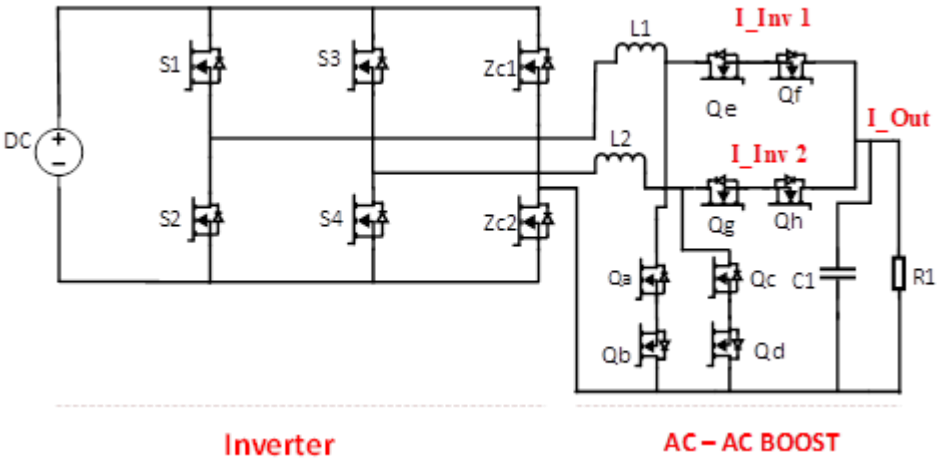

Figure 3. TP DC – AC IBI Circuit

The TP DC – AC IBI has a combined operating mode of the three-arm inverter and the AC-AC IBC on positive and negative cycles. In the positive cycle, switches S1 and S3 are active with the SPWM switching technique, switch Z C2 is active with the low-frequency PWM switching technique, switches Qa, Qc, Qf, and Qh are active with the high-frequency PWM switching technique, for switches Qb, Qd, Qe, Qg is always active, while S2, S4, and Z C1 are inactive. The following is the DC-DC IBC operating mode in the positive cycle:

- Mode 1: Power switches Qa and Qc are active. The current from Vin flows through inductors L1 and L2 via power switches S1 and S3, then returns to Vin via switch Z C2 on the inverter. In this condition, there is an increase in energy and current at L1 and L2.

- Mode 2: Qc power switch is on, Qa switch is off. Current from Vin flows through L1 and L2 via power switches S1 and S3. The current that passes through L1 will go through the power switches Qe and Qf to loads C and R. Meanwhile, the current in L2 goes through Qc and Qd. Both currents return to Vin through Z C2. In this condition, there is an increase in current at L2 and a decrease in current at L1.
- Mode 3: The Qa power switch is on, Qc switch is off. Current from Vin flows through L1 and L2 via power switches S1 and S3. The current that passes through L2 will go through the power switches Qg and Qh to loads C and R. Meanwhile, the current in L1 goes through Qa and Qb. Both currents return to Vin through Z_{C2}. In this condition, there is an increase in current at L1 and a decrease in current at L2.
- Mode 4: Power switches Qa and Qc are inactive. Current from Vin flows through L1 and L2 to the load and then returns to Vin via Z_{C2}. In this condition, the L1 and L2 currents decrease.

TP DC – AC IBI switching pattern in the positive cycle is shown in Table 2.

Table 2. TP DC – AC IBI Switching Pattern

Mode	S1	S2	S3	S4	Zc1	Zc2	A	B	C	D	E	F	G	H
1	1	0	1	0	0	1	1	1	1	1	1	0	1	0
2	1	0	0	0	0	1	0	1	1	1	1	1	1	0
3	0	0	1	0	0	1	1	1	0	1	1	0	1	1
4	0	0	1	1	0	1	0	1	0	1	1	1	1	1

2.4 Current Transducer HX – 10P

This topology uses the HX – 10P current transducer as the output current reading sensor. The reading results from the HX – 10P are the actual signal from the topology being researched. Figure 4 is a series of HX – 10P. On the primary side, there are two input pins for the output current from the TP DC – AC IBI, while on the secondary side, there are four pins, namely output, +12, GND, and -12. The advantage of the HX–10P is the high level of accuracy in reading the results.

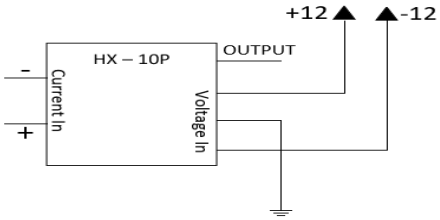

Figure 4. HX – 10P Circuit

2.5 Flow Control Strategy

Figure 5 is the output voltage control scheme used in this research. The HX—10P reading result is the actual current value, which is then compared with the reference value so that it becomes an error. The error value is processed using a Proportional Integral (PI) control strategy. The PI output sinusoidal signal is then compared with several parameters.

First, the PI output signal is compared with two triangular carrier signals that are phase-shifted by 180°, producing SPWM control signals for S1 and S3. The PI signal is also inverted and compared with the same two carrier signals to produce SPWM control signals for S2 and S4. Second, the PI output signal is compared with Ground, resulting in a PWM control signal for Zc1 and Zc2. In addition, it is also used as a switching control signal in the power circuit by inserting a high-frequency PWM signal into the logic gate circuit, thus producing a high-frequency switching signal for Qa – Qh. The entire workflow of the TP DC-AC IBI based on the description above is shown in Figure 6.

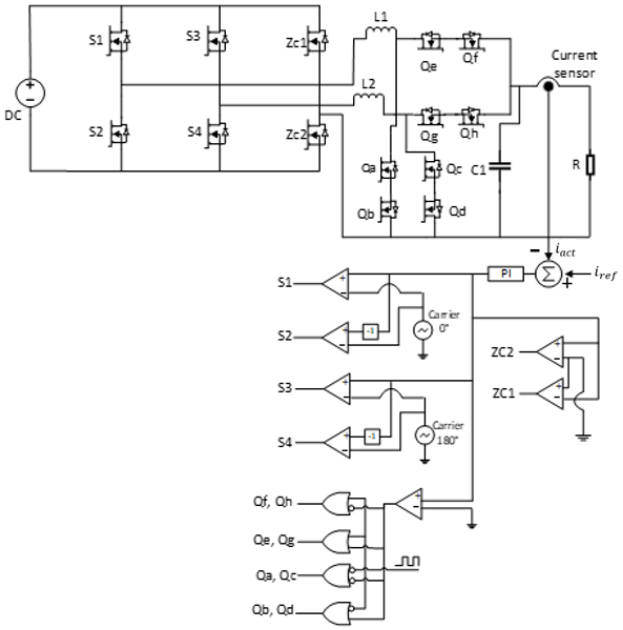

Figure 5. Current Controlled TP DC – AC IBI Strategy

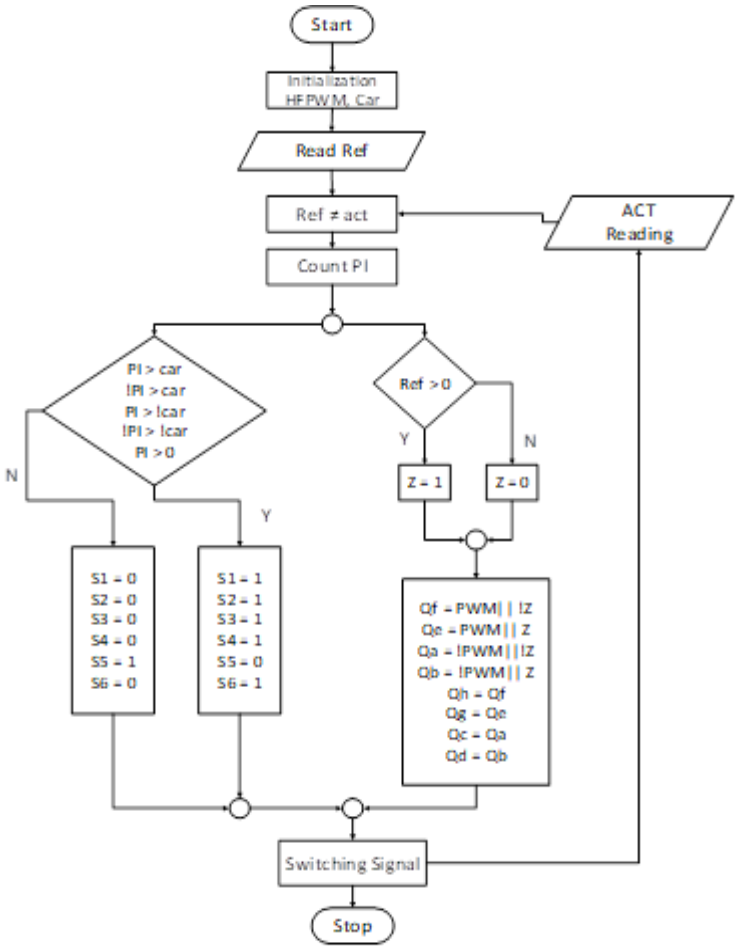

Figure 6. Flowchart of the TP DC – AC IBI

2.6 Integral Proportional Control

The topology uses a closed-loop system with PI control, which regulates the Iact value. Figure 7 is a block diagram of the PI control. PI control is a combination of proportional and integral control. The response is fast, and the

noise produced is minimal, making this control suitable for use with the topology. *Kp* is the gain value from proportional control, and *Ki* is the gain value from integrative control. The gain value is obtained by trial and error so that it can produce precise output.

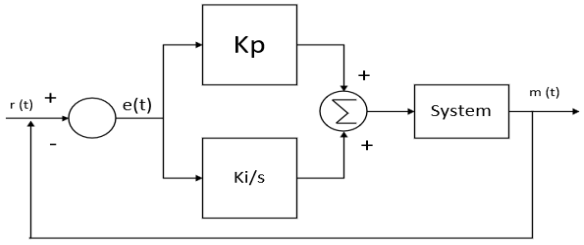

Figure 7. PI Control Block Diagram

3. Results and Discussion

Tool testing was carried out by using two methods, namely simulation and direct testing. Simulation was conducted first to test the tool until the results are as expected. Simulation testing was carried out with the help of PSIM software. Simulation testing was carried out by assembling components in the same way as the proposed design. The results obtained from the simulation were used as the reference for further testing directly (hardware). Table 3 presents several parameters recorded during tool testing.

Table 3. Measurement Parameters

Items	Value	Units
Input Voltage	50	VDC
Inductor 1	2	mH
Inductor 2	2	mH
Capacitor	47	µF
Frequency	5	K $_{HZ}$
Load	100	W

At the top, there is a series of optocouplers (TLP250) and a series of sensors for current and voltage. Meanwhile, the bottom part is the topology being researched. There is a power circuit consisting of fourteen power switches (MOSFETs), with IRFP260 as the selected series, followed by a couple of inductors, as well as capacitors and a given load. In addition, there is also other hardware to support the testing, namely an audio frequency generator (AFG) as a reference signal input, a power supply, and an oscilloscope which functions to read and display the results of the test in the form of an image of the output signal from the TP DC - AC IBI. Figure 8 is a direct implementation and test of the topology being researched.

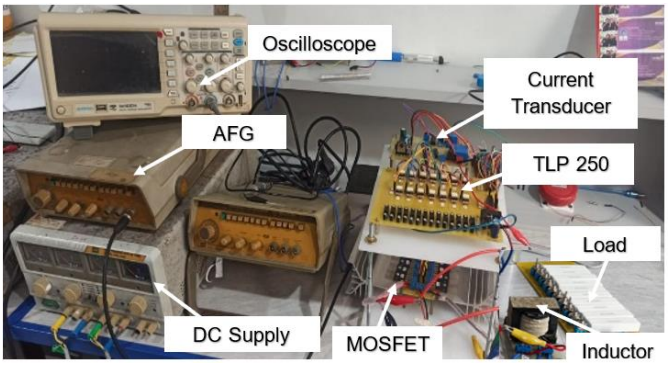

Figure 8. Implementation of the TP DC – AC IBI Hardware Design

The first test is on the output voltage section to validate that the proposed topology is in accordance with the design, namely capable of producing large power on the output side. Figure 9(a) represent the simulation test. It can be seen that the output voltage (red) is able to step up beyond the input voltage (blue). This means that the proposed topology is capable of producing large power on the output side. After that, Hardware testing was carried out, and it can be seen in Figure 9(b) that the measurement results using an oscilloscope are similar to the results obtained from the simulation.

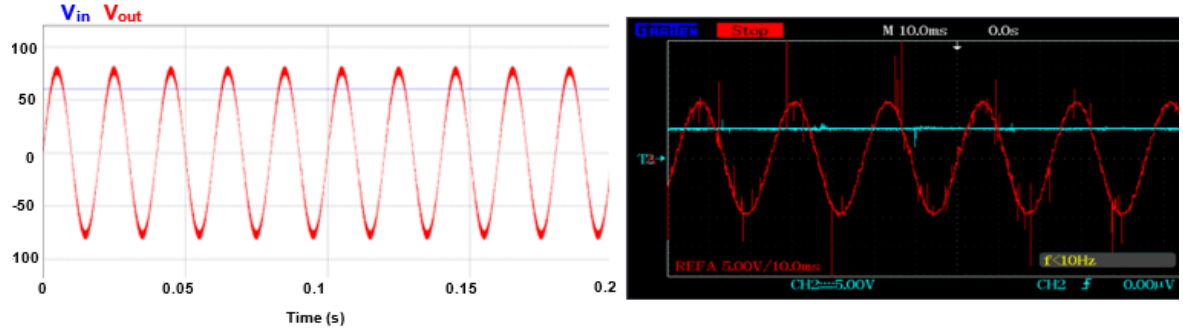

(a) (b)

Figure 9. Measurements Input and Output Voltage Side

In the next test, the data taken was the current at the output which was obtained by comparing the reference and actual current. There are two reference signals given in this topology test, namely a sine signal and a triangle signal. This aims to ensure that the proposed topology can still work as expected when given a different reference signal input. In the first currents test, a reference signal was given in the form of a sine, and the test results obtained are presented in Figure 10(a) for simulation testing, in which the reference signal (blue) and the actual signal (red) were successfully tracked. After obtaining the simulation test results, the next stage was to carry out similar tests and measurements, but the test was carried out directly (hardware). The direct test obtained similar results as in the simulation test. Figure 10(b) is the result of hardware testing where the reference signal (red) and actual signal (blue) were successfully tracked, so it can be concluded that the experiment on the current section with the sine reference signal was successful and as expected.

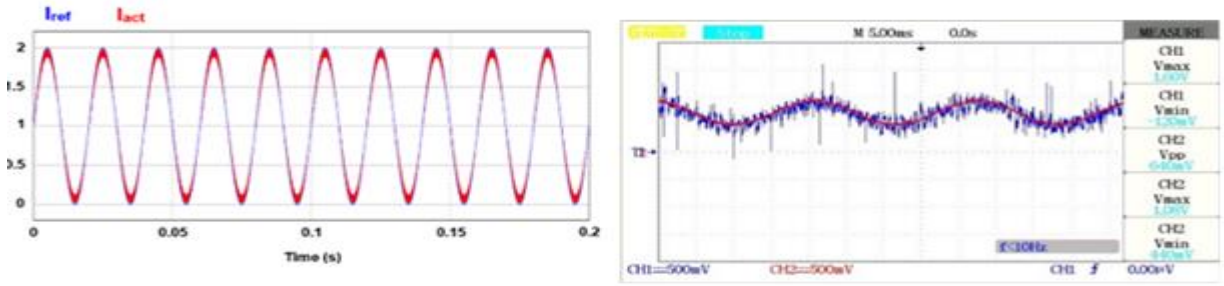

(a) (b)

Figure 10. Measurement Output Current Side with a Sine Reference

The next test was to change the shape of the reference signal to ensure that the proposed topology can work as expected. As in Figure 11(a), when the current reference signal (blue) is changed to a triangle, the actual signal (red) will follow the reference and can be declared successful. After completing the simulation, the hardware was tested with a triangular reference signal, and the proposed topology showed measurement results that were in accordance with the simulation. Figure 11(b) is the measurement result when the reference is changed to a triangle so that the actual tracking will be the same as the reference signal.

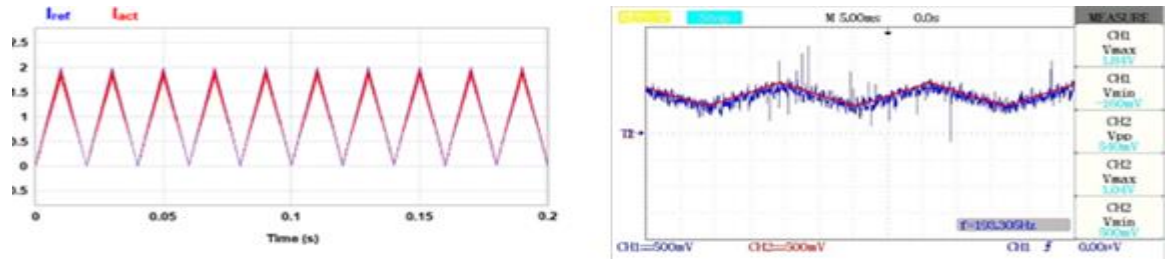

(a) (b)

Figure 11. Measurement Output Current Side with a Triangle Reference

Below is a test to prove the advantages possessed by TP DC - AC IBI. In the interleaved method, there is a couple inductors. The use of a couple inductors serves to reduce the harmonic value produced. Figure 12(a) is the

output side current using a couple inductors. It can be seen that the resulting output current signal is pure sine-shaped which means that the harmonics are successfully suppressed. Meanwhile in Figure 12(b), the output current signal shape did not use a couple inductors, so that the resulting output current signal shape is not pure sine-shaped which means that the harmonic value is still quite high.

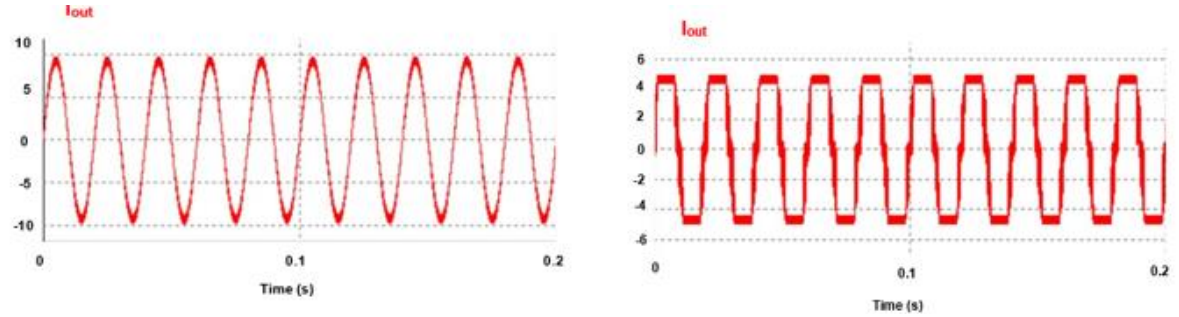

(a) (b)

Figure 12. The Advantages of the Interleaved Method

The next test was to measure THD on the output current section, which aimed to ensure that the THD of the proposed topology passed the applicable standards. Figure 13 shows the results of measuring the Total Harmonic Distortion (THD) produced by the topology. When the output current is measured, it can be seen in the picture that the resulting THD value is 3.3%. Referring to IEEE 519-2014, the obtained THD is less than 5%, which means that the proposed topology passed the standard. One way to reduce the THD value is to use an inductor couple. Low THD can minimize damage to components and extend the life of electronic components.

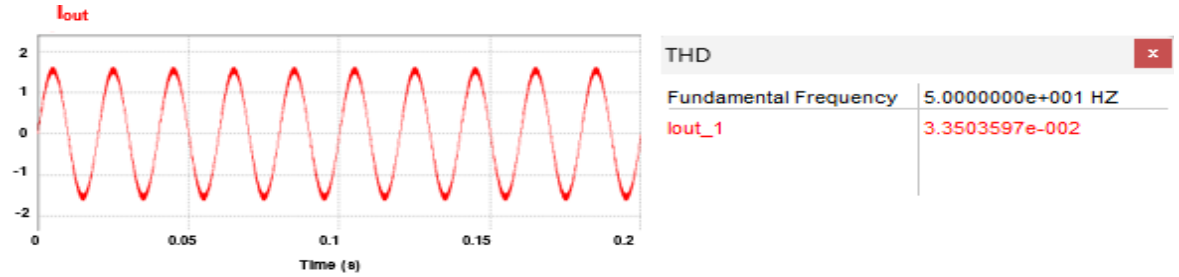

(a) (b)

Figure 13. THD Value for Output Current

The final test was the measurement of the output voltage and current. Figure 14(a) shows a simulation test in which the output current and voltage waves oscillate in one phase. After obtaining the simulation test results on the output current and voltage, the next test was carried out directly using the hardware. The measurements were carried out using an oscilloscope, and the results obtained are presented in Figure 14(b). The direct test results obtained are in accordance with the simulation test results.

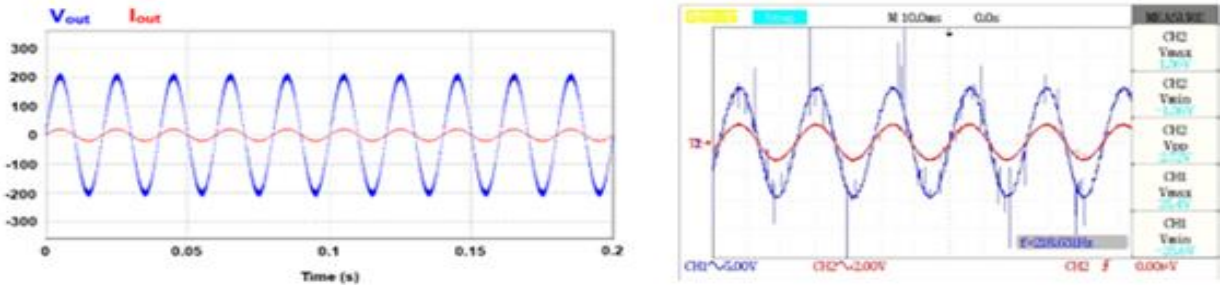

(a) (b)

Figure 14. Comparison of Output Voltage and Current

4. Conclusion

According to the analysis, computer simulations, and hardware implementations, the newly developed inverter topology (TP DC - AC IBI), functioning as a boost inverter, consistently operates effectively under the reference current.

This inverter presents multiple advantages, including a high-power output (as indicated in Equation 9) and reduced output harmonics, attributed to the utilization of 180^0 phase-shifted carrier signal modulation. The TP DC-AC IBI demonstrates a significant advantage over conventional boost inverters by effectively minimizing harmonic distortion, resulting in an output current that closely resembles a pure sine wave, making it suitable for high-power applications. To further substantiate the claim that this topology successfully reduces harmonics, total harmonic distortion (THD) measurements were conducted. The results indicated a THD value of 3.3% on the output current side of this configuration. This THD value passed the permissible limit of less than 5% as stipulated by relevant IEEE standards. This topology presents advantages that make it appropriate for application in electrical systems, especially in the field of new and renewable energy. Nevertheless, the TP DC - AC IBI inverter is not without its drawbacks, as it employs numerous power switches, which contributes to power losses. Consequently, it does not achieve near-perfect efficiency and incurs significant costs.

References

[1] W. Zhang, Y. Wang, P. Xu, D. Li, and B. Liu, “A Current Control Method for Grid-Connected Inverters,” *Energies* , vol. 16, no. 18, 2023, https://doi.org/10.3390/en16186558

[2] P. Mao, M. Zhang, S. Cui, W. Zhang, and BH Kwon, “A review of current control strategies for single-phase grid-connected inverters,” *Telkomnika (Telecommunication Comput. Electron. Control.* , vol. 12 , no. 3, pp. 563–580, 2014, https://doi.org/10.12928/v12i3.94

[3] SANDEEP KOLLURI NVML, "Analysis, Design and Implementation of an Auxiliary Current Pump Module for Improved Load Transient Response of Battery Discharge Regulator," INDIAN INSTITUTE OF TECHNOLOGY MADRAS., 2014.

[4] AG Pratama, "DESIGN AND IMPLEMENTATION OF INTERLEAVED BOOST CONVERTER FOR PHOTOVOLTAIC MODULE APPLICATION," Sepuluh Nopember Institute of Technology, 2015.

[5] S. Nahar and M. Bashir Uddin, “Analysis of the performance of interleaved boost converters,” *4th Int. Conf. Electr. Eng. Inf. Commun. Technol. iCEEiCT 2018* , vol. 8, pp. 547–551, 2018. https://doi.org/10.1109/ceeict.2018.8628104

[6] Sunarno et al., “A simple and implementation of interleaved boost converter for renewable energy,” Proc. - 6th Int. Conf. Sustain. Energy Eng. Appl. ICSEEA 2018, no. 1, pp. 75–80, 2019. https://doi.org/10.1109/icseea.2018.8627094

[7] Y. Zhang, H. Liu, J. Li, M. Sumner, and C. Xia, “DC-DC Boost Converter with a Wide Input Range and High Voltage Gain for Fuel Cell Vehicles,” *IEEE Trans. PowerElectron.* , vol. 34, no. 5, pp. 4100–4111, 2019. https://doi.org/10.1109/tpel.2018.2858443

[8] Indragandhi, V. Subramaniyaswamy, and R. Logesh, “Topological review and analysis of DC-DC boost converters,” *J. Eng. Sci. Technol.* , vol. 12, no. 6, pp. 1541–1567, 2017.

[9] Alhamrouni, N. Zainuddin, M. Salem, NHA Rahman, and L. Awalin, "Design of single phase inverter for photovoltaic applications controlled with sinusoidal pulse width modulation," *Indonesia. J. Electr. Eng. Comput. Sci.*, vol. 15, no. 2, pp. 620–630, 2019. https://doi.org/10.11591/ijeecs.v15.i2.pp620-630

[10] M. Y. Hammoudi, O. Kraa, R. Saadi, M. Y. Ayad, S. Bacha, and A. Boukhlouf, “Non linear control of a Fuel Cell Interleaved Boost Converter using Weighted Mixed Sensitivity H∞,” *Proc. 2018 3rd Int. Conf. Electr. Sci. Technol. Maghreb, Cist. 2018*, pp. 1–5, 2018, https://doi.org/10.1109/CISTEM.2018.8613563.

[11] R. Priya and R. Valli, “Advanced multilevel inverter techniques for PV applications with reduced switching devices and THD with voltage balancing,” *2019 IEEE Int. Conf. Syst. Comput. Autom. Networking, ICSCAN 2019*, pp. 1–8, 2019, https://doi.org/10.1109/ICSCAN.2019.8878702.

[12] V. Indragandhi, V. Subramaniyaswamy, and R. Logesh, “Topological review and analysis of DC-DC boost converters,” *J. Eng. Sci. Technol.*, vol. 12, no. 6, pp. 1541–1567, 2017.

[13] RB Kananthoor and BA Rao, “Interleaved boost converter,” *Int. J. Elec&Electr.Eng&Telecoms. 2015 ISSN 2319 – 2518*, vol. 1, no. 1, pp. 305–310, 2015.

[14] N. Shanthi, P. Nivethitha, S. Sindhuja, M. Hilasini, and K. Divyabharathi, “High Efficient Interleaved Boost Converter for Photovoltaic Applications,” *7th IEEE Int. Conf. Comput. Power, Energy, Inf. Commun. ICCPEIC 2018*, pp. 305–308, 2018. https://doi.org/10.1109/ICCPEIC.2018.8525145

[15] H. Wu, T. Mu, H. Ge, and Y. Xing, “Full-Range Soft-Switching-Isolated Buck-Boost Converters with Integrated Interleaved Boost Converter and Phase-Shifted Control,” *IEEE Trans. PowerElectron.* , vol. 31, no. 2, pp. 987–999, 2016. https://doi.org/10.1109/TPEL.2015.2425956

[16] AV Deshpande, BK Patil, RB Magadum, and NR Chitragar, “Design and Simulation of Interleaved Boost Converter,” *2021 Int. Conf. Syst. Comput. Auto. Networking, ICSCAN 2021* , no. January, 2021. https://doi.org/10.1109/ICSCAN53069.2021.9526469

[17] M. Muhammad, M. Armstrong, and M.A. Elgendy, “A Nonisolated Interleaved Boost Converter for High-Voltage Gain Applications,” *IEEE J. Emerg. Cell. Top. PowerElectron.* , vol. 4, no. 2, pp. 352–362, 2016. https://doi.org/10.1109/JESTPE.2015.2488839

[18] N. Rana, S. Banerjee, SK Giri, A. Trivedi, and SS Williamson, “Modeling, analysis and implementation of an improved interleaved buck-boost converter,” *IEEE Trans. Circuits Syst. II Express Briefs* , vol. 68, no. 7, pp. 2588–2592, 2021. https://doi.org/10.1109/TCSII.2021.3056478

[19] M. Sharma, A. Achra, V. Gali, and M. Gupta, “Design and Performance Analysis of Interleaved Inverter Topology for Photovoltaic Applications,” *2020 Int. Conf. Power Electron. IoT Appl. Renew. Energy its Control. PARC 2020*, pp. 180–185, 2020, https://doi.org/10.1109/PARC49193.2020.236589

[20] E. Kabalci and A. Boyar, “Design and Analysis of Two-phase Interleaved Boost Converter and H5 Inverter Based Microinverter,” *Proc. - 2019 IEEE 1st Glob. Power, Energy Commun. Conf. GPECOM 2019*, pp. 122–127, 2019, https://doi.org/10.1109/GPECOM.2019.8778497

[21] A. Roy and A. Ghosh, “Multistage Feedback Control of a PV Supplied Two Phase Interleaved Boost Converter for Grid Interfacing Applications,” *2021 Int. Conf. Nascent Technol. Eng. ICNET 2021 - Proc.*, no. Icnte, 2021, https://doi.org/10.1109/ICNTE51185.2021.9487727

[22] S. Christian, R. A. Fantino, R. Amir Gomez, Y. Zhao, and J. C. Balda, “Variable-Frequency Controlled Interleaved Boost Converter,” *ECCE 2020 - IEEE Energy Convers. Congr. Expo.*, pp. 601–606, 2020, https://doi.org/10.1109/ECCE44975.2020.9235926

[23] G. Liu, W. Zhou, Q. Wu, Y. Fu, and M. Wang, “A Sensorless Current Balance Control Method for Interleaved Boost Converter,” *Conf. Proc. - IEEE Appl. Power Electron. Conf. Expo. - APEC*, vol. 2020-March, pp. 3019–3023, 2020, https://doi.org/10.1109/APEC39645.2020.9124340.

[24] M. Veerachary, “Switched L-C cell based interleaved boost converter,” *9th IEEE Int. Conf. Power Electron. Drives Energy Syst. PEDES 2020*, pp. 0–4, 2020, https://doi.org/10.1109/PEDES49360.2020.9379577.